

Effect of speed humps on instantaneous traffic emissions in a microscopic model with limited deceleration capacity

Yu-Chen Hu(胡宇晨), Qi-Lang Li(李启朗), Jun Liu(刘军), Jun-Xia Wang(王君霞), and Bing-Hong Wang(汪秉宏)
Citation: Chin. Phys. B, 2024, 33 (**6**): 064501. DOI: 10.1088/1674-1056/ad2608
Journal homepage: http://cpb.iphy.ac.cn; http://iopscience.iop.org/cpb

What follows is a list of articles you may be interested in

Efficient control of connected and automated vehicles on a two-lane highway with a moving bottleneck

Huaqing Liu(刘华清) and Rui Jiang(姜锐)
Chin. Phys. B, 2023, 32 (**5**): 054501. DOI: 10.1088/1674-1056/acb918

A stochastic two-dimensional intelligent driver car-following model with vehicular dynamics

Hong-Sheng Qi(祁宏生) and Yu-Yan Ying(应雨燕)
Chin. Phys. B, 2023, 32 (**4**): 044501. DOI: 10.1088/1674-1056/ac8f3c

Traffic flow of connected and automated vehicles at lane drop on two-lane highway: An optimization-based control algorithm *versus* a heuristic rules-based algorithm

Huaqing Liu(刘华清), Rui Jiang(姜锐), Junfang Tian(田钧方), and Kaixuan Zhu(朱凯旋)
Chin. Phys. B, 2023, 32 (**1**): 014501. DOI: 10.1088/1674-1056/ac9369

A modified heuristics-based model for simulating realistic pedestrian movement behavior

Wei-Li Wang(王维莉), Hai-Cheng Li(李海城), Jia-Yu Rong(戎加宇), Qin-Qin Fan(范勤勤), Xin Han(韩新), and Bei-Hua Cong(丛北华)
Chin. Phys. B, 2022, 31 (**9**): 094501. DOI: 10.1088/1674-1056/ac65f8

Modeling the heterogeneous traffic flow considering the effect of self-stabilizing and autonomous vehicles

Yuan Gong(公元) and Wen-Xing Zhu(朱文兴)
Chin. Phys. B, 2022, 31 (**2**): 024502. DOI: 10.1088/1674-1056/ac2b18

Effect of speed humps on instantaneous traffic emissions in a microscopic model with limited deceleration capacity

Yu-Chen Hu(胡宇晨)[1], Qi-Lang Li(李启朗)[1,†], Jun Liu(刘军)[1], Jun-Xia Wang(王君霞)[2], and Bing-Hong Wang(汪秉宏)[3]

[1] *School of Mathematics and Physics, Anhui Jianzhu University, Hefei* 230601, *China*
[2] *School of Civil Engineering and Transportation, Northeast Forestry University, Harbin* 150040, *China*
[3] *Department of Modern Physics, University of Science and Technology of China, Hefei* 230026, *China*

(Received 16 November 2023; revised manuscript received 17 January 2024; accepted manuscript online 5 February 2024)

As a common transportation facility, speed humps can control the speed of vehicles on special road sections to reduce traffic risks. At the same time, they also cause instantaneous traffic emissions. Based on the classic instantaneous traffic emission model and the limited deceleration capacity microscopic traffic flow model with slow-to-start rules, this paper has investigated the impact of speed humps on traffic flow and the instantaneous emissions of vehicle pollutants in a single lane situation. The numerical simulation results have shown that speed humps have significant effects on traffic flow and traffic emissions. In a free-flow region, the increase of speed humps leads to the continuous rise of CO_2, NO_X and PM emissions. Within some density ranges, one finds that these pollutant emissions can evolve into some higher values under some random seeds. Under other random seeds, they can evolve into some lower values. In a wide moving jam region, the emission values of these pollutants sometimes appear as continuous or intermittent phenomenon. Compared to the refined NaSch model, the present model has lower instantaneous emissions such as CO_2, NO_X and PM and higher volatile organic components (VOC) emissions. Compared to the limited deceleration capacity model without slow-to-start rules, the present model also has lower instantaneous emissions such as CO_2, NO_X and PM and higher VOC emissions in a wide moving jam region. These results can also be confirmed or explained by the statistical values of vehicle velocity and acceleration.

Keywords: traffic emissions, speed humps, slow-to-start rules, deceleration capacity

PACS: 45.70.Vn **DOI:** 10.1088/1674-1056/ad2608

1. Introduction

In recent years, with the rapid development of the national economy and the steady advancement of urbanization, the transportation system has been continuously improved, which has greatly facilitated people's ability to travel and has improved road traffic capacity. At the same time, due to the long-term existence of problems such as lagging construction of related transportation facilities and unreasonable road planning, its negative effects are becoming increasingly serious. The continuous increase of vehicles on the road leads to the emission of motor vehicle pollutants becoming one of the main sources of air pollution in major and medium-sized cities, which poses a great threat to human health and the ecological environment.[1–5]

It is well-known that the power of a vehicle comes from the fuel combustion within the engine; this process is not perfect. Therefore, exhaust gas is inevitably discharged. The emission of automobile pollutants has become a hot issue in the field of environmental research. Contaminants include carbon dioxide (CO_2), hydrocarbons (HC), particulate matter (PM), nitrogen oxides (NO_X), volatile organic components (VOC), etc. In fact, PM concentration is a key parameter to characterize air quality. The exhaust emissions of road vehicles account for more than half of the total PM emissions in urban areas, and in some metropolises in developed countries, the proportion even exceeds 80%.[5–7] CO_2 is also one of the main gases that cause global warming; automobile exhaust emissions account for about 17% of HC and 23% of CO_2 emissions, anthropogenic carbon emissions behaviors have accelerated the process of global warming and seriously threaten the sustainable development of human society and ecosystems.[8–11] In addition, a large amount of NO_X produced by automobile exhaust emissions forms ozone (O_3) after chemical reaction with VOC, which is an important factor causing regional composite pollution.[11–13]

Speed humps are traffic facilities installed on the road to force vehicles to slow down and they are widely used, being easy to install and low cost.[14] Installing a speed hump is an effective measure to adjust vehicle speed and improve pedestrian and driving safety. At present, there are some studies on the impact of speed humps on road traffic accidents and vehicle energy consumption. Obeng *et al.*[15] explored whether speed humps play a role in the deceleration behavior of vehicles by using some of the main roads of the expressway, and proved that the accident rate can be effectively reduced by setting its position and distribution spacing reasonably. Has-

†Corresponding author. E-mail: qlli@ahjzu.edu.cn

© 2024 Chinese Physical Society and IOP Publishing Ltd

souna *et al.*[16] used the energy-harvesting speed hump system as an alternative to traditional speed humps, hoping to reduce greenhouse gas emissions. Zhou *et al.*[17] established a nonlinear vehicle dynamics model, which provides a new speed optimization method for autonomous vehicles to alleviate the reduction of driving comfort caused by the installation of road speed humps. Obregón-Biosca[18] reduces the maximum speed of vehicles between speed humps by redesigning the shape, size and height of the speed humps, effectively reducing the fuel consumption of vehicles. However, there are few studies on the impact of speed humps on road vehicle emissions.[18–20] Based on a refined limited deceleration capacity microscopic traffic flow model with slow-to-start rules, this paper examines the effects of different numbers of speed humps on vehicle pollutant emissions, including CO_2, NO_X, PM and VOC, road traffic flow and so on.

2. Previous works

Cellular automata is one of the mainstream methods to study the characteristics of road traffic flow. In 1992, Nagel and Schreckenberg[21] proposed the classical NaSch model. Afterward, researchers extended many complex new models based on its update rules and applied them to study various characteristics of traffic flow.[22–30] The cellular automata traffic flow model is suitable for the simulation of a real road traffic system because of its flexible evolution rules, high computational efficiency and the ability to reproduce many dynamic characteristics of complex traffic flow systems.[31–34]

Nowadays, an investigation using the cellular automata model to simulate vehicle pollutant emissions is mainly based on the combination of the NaSch model[35–38] and the instantaneous traffic emission model.[39–43] Madani and Moussa[35] simulated the fuel consumption and gas emissions of the NaSch model and its improved model under periodic boundary conditions. Xue *et al.*[37] studied the emission of various pollutants based on the NaSch model and instantaneous emission formula, considering different driving conditions, vehicle mixing ratio, maximum speed and other factors. Pan *et al.*[38] simulated the energy consumption and particulate matter emissions at a road traffic bottleneck of the NaSch model. Xue *et al.*[42] also studied the particulate matter emissions of two cellular automata models with slow-to-start rules. However, there are few studies on the cellular automata model considering the effect of speed humps on air quality and pollutant emissions[43,44] In 2006, Meng and Zhang[43] introduced the concept of speed humps into the cellular automata model. By modifying the deceleration rule of the NaSch model, they simulated the negative impact of installing speed humps on traffic flow and vehicle speed under a fixed road length. On this basis, Pérez-Sansalvador*et al.*[44] further explored the impact of setting different numbers of speed humps on vehicle pollutant emissions on a single lane. These studies on speed humps were carried out under the NaSch model update rules, which are easy to understand but are indeed too simple. Is the effectiveness of speed humps still obvious when simulating vehicle pollution emissions in other more complex cellular automata models?

Moreover, based on the Lee model,[28] Pottmeier *et al.*[29] set more rigorous conditions for the establishment of man-made overreaction, introduced brake lights,[26,27] and proposed a new Pottmeier model. Due to the fact that the vehicle engine starts slowly, the complex urban road conditions, and the driver's inattention in the actual traffic, a certain type of slow-to-start rule in the cellular automata model is considered to be applied to the deceleration model. Slow-to-start rules can cause phase transition in the metastable traffic flow with a certain probability, which makes the traffic flow spontaneously change from metastable free flow or synchronous flow to clogged flow.[30,45] In order to simulate the delay when vehicles restart, that is, due to the loss of the driver's attention or the slow start of the engine, Li *et al.*[46] proposed a traffic flow model with limited deceleration capacity considering the slow-to-start rules of the Takayasu and Takayasu (TT) model[23,24] on the basis of the Pottmeier's model, emphasizing that the limited dynamic capacity of vehicles and human overreaction are the root causes of traffic congestion. In general, the traditional cellular automata traffic flow model cannot reproduce the synchronous flow in the three-phase traffic flow theory, but this model can well reproduce the three different phases of traffic flow (free flow, synchronous flow and wide moving jam) and two first-order phase transitions (phase transition from free flow to synchronous flow and phase transition from synchronous flow to wide moving jam) under periodic boundary conditions, and the phase transition from synchronous flow to wide moving jam is very obvious. In this paper, the limited deceleration capacity microscopic traffic flow model with slow-to-start rules is further proposed.

3. Description of the present model

3.1. The limited deceleration capacity model with slow-to-start rules

The specific vehicle update rules of the limited deceleration capacity model with slow-to-start rules are as follows:

1. The randomization parameter p:

$$p = \max\left\{p_{\mathrm{d}}, p_0 - v_n^t(p_0 - p_{\mathrm{d}})/v_{\mathrm{slow}}\right\}.$$

2. Deceleration caused by speed humps: If the driver finds that there is a speed hump on the road ahead, and the vehicle can reach the position of the speed hump at least in one time step, this vehicle will start to slow down and move

upstream closest to the speed hump. When the vehicle is partially through the speed hump or completely on it, the speed of the vehicle will be reduced to a fixed minimum. If another vehicle does not pass and occupy the speed hump in the next time step, the deceleration behavior of this vehicle is not related to this speed hump.

$$\begin{cases} v_n^{t+1} = \min(D_{\rm d}, d_n - L_{\rm vehicle}) & \text{if } D_{\rm d} > 4 \text{ and } D_{\rm d} \le v_n^t; \\ v_n^{t+1} = \min(5, d_n - L_{\rm vehicle}) & \text{if } 1 \le D_{\rm d} \le 4 \text{ or } D_{\rm d} = 0; \\ v_n^{t+1} = \min(v_n^t, d_n - L_{\rm vehicle}) & \text{otherwise.} \end{cases}$$

3. The maximal safe velocity: $\tilde{c}_n^{t+1} = \max\{c_n^{t+1} \mid c_n^{t+1}$ satisfies Eqs. (1)–(3) $\}$.

4. Velocity update: if $v_n^t = 0$ and its gap $= 1$, then $\tilde{v}_n^{t+1} = 0$ with $p_t = 0.75$. For other cases, $\tilde{v}_n^{t+1} = \min(v_{\max}, v_n^{t+1} + a, \max\{0, v_n^{t+1} - D, \tilde{c}_n^{t+1}\})$.

5. Randomization: $v_n^{t+1} = \max\{0, v_n^t - D, \tilde{v}_n^{t+1} - \eta\}$, if rand$() < p, \eta = 1$, otherwise $\eta = 0$.

6. Vehicle movement: $x_n^{t+1} = x_n^t + v_n^{t+1}$.

Here, the values of each parameter are consistent with the setting in Ref. [29]. The stochastic parameter p (< 1) in step (i) linearly interpolates between p_0 and $p_{\rm d}$. The parameters $p_0 = 0.32$, $p_{\rm d} = 0.11$ and $v_{\rm slow} = 5$. v_n^t and x_n^t represent the speed and headway position of the nth vehicle (the current vehicle) at time step t, $v_{\max}$ represents the maximum speed allowed by the road vehicle, $L_{\rm vehicle}$ represents the length of the vehicle, gap represents the distance between the nth car and the $n+1$th car (the front car) at time t, p_t is the probability that the vehicle stays in place in the next time step in the update rule of the extended TT model.[24] Pérez-Sansalvador *et al.*[44] take a fixed value of 1 when $v_{\max} = 4$, while $v_{\max} = 20$ in the Pottmeier model, so the value is 5 in our study. $D_{\rm d}$ represents the distance between the current vehicle and the nearest speed hump l in front of it $(D_{\rm d} = x_l^t - x_n^t)$. d_n denotes the distance between the nth vehicle and the $n+1$th vehicle (the preceding vehicle) at time t, which includes the length of the vehicle $(d_n = x_{n+1}^t - x_n^t)$. D is the maximum deceleration.

The safe driving speed of the next time step ($t+1$ time step) is represented by c_n^{t+1}, which satisfies the following formula:

$$x_n^t + \Delta + \sum_{i=0}^{\tau_f(c_n^{t+1})} (c_n^{t+1} - Di) \le x_{n+1}^t + \sum_{i=1}^{\tau_l(v_{n+1}^t)} (v_{n+1}^t - Di), \quad (1)$$

where τ_f and τ_l represent the time steps required for the nth vehicle and the $n+1$th vehicle to continue to decelerate until they stop completely, respectively. Accumulation represents the sum of the vehicles at time steps $i = 0, 1, \ldots, \tau_f/\tau_l$. Δ represents the minimum distance between the current vehicle and the preceding vehicle, which is at least the length of the vehicle. The expressions of τ_f, τ_l and Δ are as follows:

$$\begin{cases} \Delta = l + \gamma_n^t \times \max\{0, \min[g_{\rm add}, v_n^t - g_{\rm add}]\}, \\ \tau_f(v) = \gamma_n^t \times v/D + (1-\gamma_n^t) \times \max\{0, \min[v/D, t_{\rm safe}] - 1\}, \\ \tau_l(v) = \gamma_n^t \times v/D + (1-\gamma_n^t) \times \min\{v/D, t_{\rm safe}\}, \end{cases} \quad (2)$$

where $g_{\rm add}$ represents the additional safety distance required when the following vehicle (current vehicle) is in a pessimistic state. $t_{\rm safe}$ represents the maximum time steps that the following vehicle can predict that it is in a safe state when driving optimistically. The binary variable γ_n^t reflects the driver's biased behavior towards local traffic conditions. $\gamma_n^t = 0$ indicates that the driver is optimistic about the road condition because the vehicle in front is accelerating, $\gamma_n^t = 1$ means that the driver is pessimistic, and the vehicle needs to drive below the safe speed. The definition of γ_n^t is as follows:

$$\gamma_n^t = \begin{cases} 0, & \text{for } (v_n^t \le v_{n+1}^t < v_{n+2}^t) \text{ or} \\ & (v_{n+2}^t \ge v_{\rm fast} \cap v_n^t - v_{n+1}^t \le D \cap b_{n+2}^t = 0), \\ 1, & \text{otherwise.} \end{cases} \quad (3)$$

3.2. The instantaneous traffic emission model

This study will adopt the instantaneous traffic emission model proposed by Panis *et al.*[39] By using the nonlinear multivariate regression technique and the measured data of road vehicles, an empirical emission model related to vehicle speed and acceleration is obtained, which describes instantaneous traffic emissions as a function of pollutant emissions under different vehicle types. The formula of the emission model is

$$\begin{aligned} E_n(t) = \max\big[&E_0, f_1 + f_2 v_n(t) + f_3 v_n^2(t) \\ &+ f_4 a_n(t) + f_5 a_n^2(t) + f_6 v_n(t) a_n(t)\big], \end{aligned} \quad (4)$$

where $v_n(t)$ in Eq. (4) is the speed of the nth vehicle after randomization in the present model shown in step v in Subsection 3.1 (namely, v_n^{t+1}), $a_n(t)$ is the acceleration, that is, the difference between the speed of the vehicle after randomization and the speed of the vehicle in the previous time step $(a_n(t) = v_n^{t+1} - v_n^t)$. The unit of speed and acceleration is m/s and m/s^2, and the unit of pollutant emission is g/s. E_0 represents the minimum emission of pollutants from different types of vehicles, which is usually zero. f_1 to f_6 represent the emission coefficients. For the emission of various pollutants from different types of vehicles, the emission coefficients are different.[43,44] Since the vast majority of vehicles in actual traffic are gasoline vehicles, for the sake of simplicity, only gasoline vehicles are considered in this study, which can effectively avoid the differences caused by different types of vehicles.[44] Table 1 lists the emission coefficient values of gasoline vehicles.

Table 1. Gasoline vehicle emission coefficients are selected from Ref. [39].

Pollutant	E_0	f_1	f_2	f_3	f_4	f_5	f_6
CO_2	0	5.53×10^{-1}	1.61×10^{-1}	-2.89×10^{-3}	2.66×10^{-1}	5.11×10^{-1}	1.83×10^{-1}
NO_X ($a\geq-0.5$ m/s^2)	0	6.19×10^{-4}	8.00×10^{-5}	-4.03×10^{-6}	-4.13×10^{-4}	3.80×10^{-4}	1.77×10^{-4}
NO_X ($a<-0.5$ m/s^2)	0	2.17×10^{-4}	0	0	0	0	0
VOC ($a\geq-0.5$ m/s^2)	0	4.47×10^{-3}	7.32×10^{-7}	-2.87×10^{-8}	-3.41×10^{-6}	4.94×10^{-6}	1.66×10^{-6}
VOC ($a<-0.5$ m/s^2)	0	2.63×10^{-3}	0	0	0	0	0
PM	0	0	1.57×10^{-5}	-9.21×10^{-7}	0	3.75×10^{-5}	1.89×10^{-5}

4. Simulation result of the present model

In the present model, the single lane L_{road} is composed of 40000 cells and the length of each cell is 1.5 m. Thus, this single lane is equivalent to an actual road length of 60 km. Moreover, the length of the vehicle and the speed hump are both 7.5 m, that is, each vehicle and speed hump occupy five consecutive cells. The total number of vehicles remains unchanged under the periodic boundary condition. At first, all the vehicles are evenly distributed on single-lane roads. A total of 50 independent tests are carried out. Each test run has 40000 time steps, and the last 10000 time steps are taken to calculate the corresponding values. Each time step corresponds to 1 s in reality. The speed humps are also evenly distributed on the road. The distance between any two adjacent speed humps is $L_{\text{road}}/N_{\text{dec}}$, where N_{dec} represents the number of speed humps.

4.1. The impact of speed humps on traffic flow and vehicle velocity

This section will study the effect of speed humps on the traffic flow and vehicle speed. Figure 1(a) presents the fundamental diagram (FD) under different numbers of speed humps. In this figure, it can be seen that there are three typical phases: free flow, synchronized flow and wide moving jam. In the free-flow region ($0<d<d_{\text{FS}}$), it can be noted that the graph of the flow with the density under different numbers of speed humps overlaps and increases linearly. The movement of vehicles does not affect each other, and they have enough spatial distance to maintain high speed, as shown in Fig. 1(b). Whether the distribution of speed humps is dense or not has little effect on the overall traffic flow; the traffic flow is almost unchanged under different numbers of speed humps. In the density range ($d_{\text{FS}}\leq d<d_{\text{SJB}}$), the system can self-organize and evolve into a synchronized flow. In this synchronized flow region, almost all vehicles can still maintain medium or high speed movement while driving. With the increase of density, especially in the density range ($d_{\text{SJF}}\leq d<d_{\text{SJB}}$), these flow curves under different speed humps ultimately reach the same peak value of 1450 veh/h under some random seeds. Under other random seeds, the system can also self-organize and evolve into a wide moving jam. In a wide moving jam, the difference between the normal speed of a vehicle and its speed when passing through a speed hump will decrease as the density increases. That is to say, speed humps have little effect on the speed of vehicles passing through them in this region. In short, speed humps only have an impact on the traffic flow and speed within the synchronous flow region.

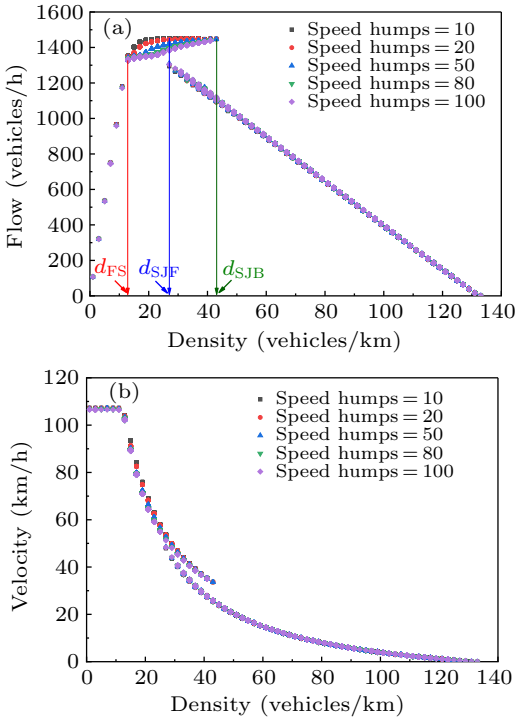


Fig. 1. Fundamental diagram of the present model.

4.2. The impact of speed humps on instantaneous traffic emission

This section shows the impact of speed humps on the emission of various pollutants. Figures 2(a)–2(c) show the relationship between CO_2, NO_X and PM emissions and density under different numbers of speed humps. In a free-flow region, when a certain number of speed humps are set on the road, these emissions slightly increase or remain unchanged with the increase of vehicle density, that is, the increase in emissions caused by the increase in density is very limited. However, one finds that the value of these pollutant emissions is increased by the increase in the number of speed humps. In

a synchronous flow region, except for the fewer speed humps in Fig. 2(a), the CO_2, NO_X and PM emissions under different speed humps first increase, gradually reach their respective maximum values, and finally gradually decrease to the same value as the vehicle density increases. One also finds that the value of these pollutant emissions is increased by the increase in the number of speed humps for some given density. Within this range $d_{\mathrm{SJF}} \leq d < d_{\mathrm{SJB}}$, the system can evolve into synchronized flow under some random seeds; one finds that there are high emission values of various pollutants in Figs. 2(a)–2(c). This is because speed humps have an inhibiting effect on the speed of vehicles on the road, and these vehicles have to accelerate or slow down frequently when passing through speed humps, which leads to an increase in pollutant emissions in the system. Under other random seeds, the system can evolve into a wide moving jam and there are relatively low emission values of various pollutants, as shown in Figs. 2(a)–2(c). The vehicles that form a wide moving jam in the system do not need to accelerate or decelerate frequently when passing through speed humps. This is because these vehicles themselves have very low speeds. In addition, it can be noted that the emission values of these pollutants appear sometimes as continuous or intermittent phenomenon in a high density wide moving jam region.

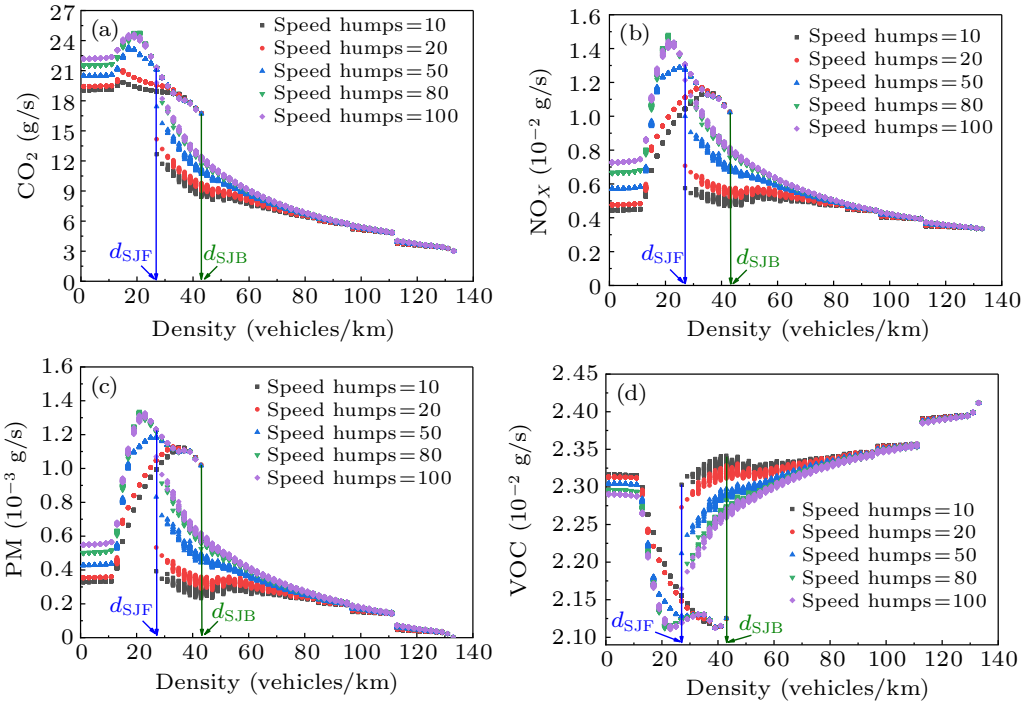


Fig. 2. Instantaneous emissions of the present model with different pollutants. (a) CO_2, (b) NO_X, (c) PM, (d) VOC.

Figure 2(d) shows the relationship between VOC emission and density under a different number of speed humps. It can be found that the emission characteristics of pollutant VOC are the opposite of the three emission characteristics discussed above. In a free-flow region, the value of these pollutant emissions is decreased by the increase in the number of speed humps for some given density. In a synchronous flow region, the VOC emissions under different speed humps first decrease, gradually reach their respective minimum values, and finally gradually increase to the same value as the vehicle density increases. It should be noted that there are two minimum values for pollutant emissions in the system. Similarly, in this region ($d_{\mathrm{SJF}} \leq d < d_{\mathrm{SJB}}$) where synchronized flow and wide moving jam coexist, the emission value of pollutants has two values depending on the random seeds, and these emission values are also decreased by the increase in the number of speed humps for some given density. In a wide moving jam, the VOC emissions under different speed humps gradually increase to the same value as the vehicle density increases. It can be noted that the emission values of these pollutants also appear sometimes as continuous or intermittent phenomenon in high density regions.

4.3. Statistical distribution of velocity and acceleration

Due to the fact that the changing trend of the curve of instantaneous emissions with vehicle density is basically the same under various numbers of speed humps, we take speed humps = 10 as an example. Figure 3 shows the statistical distribution of vehicle speed and acceleration in synchronous flow and a wide moving jam region. In these two regions, the proportion of these vehicles where their speeds are equal to zero rapidly increases with the increase of density, as shown

in Figs. 3(a), 3(c) and 3(e). Meanwhile, the proportion of these vehicles with their speeds equal to zero has exceeded half the total number of vehicles in Figs. 3(c) and 3(e). Similarly, the proportion of these vehicles whose acceleration values are equal to zero increases rapidly with increasing density, as shown in Figs. 3(b), 3(d) and 3(f). According to Eq. (4) of the instantaneous emission model, the instantaneous emissions of pollutants such as CO_2, NO_X, and PM are simultaneously reduced, as shown in Figs. 2(a), 2(b) and (c). This is because there are more and more vehicles whose speed and acceleration values are equal to zero, and their local traffic jams can gradually evolve into large-scale traffic jams. Meanwhile, the increasingly serious road congestion leads to the increase of local air circulation and the increase of VOC emissions inside the vehicle, as shown in Fig. 2(d).

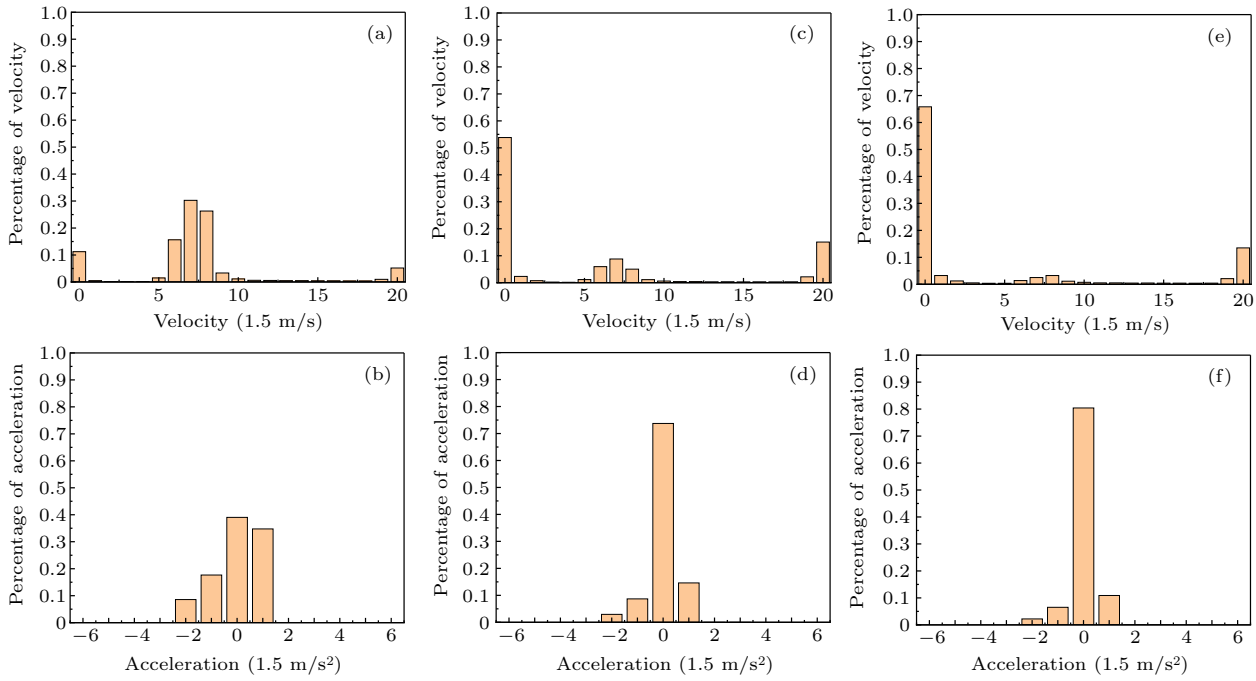


Fig. 3. Histogram of statistical distribution of velocity and acceleration of the present model. (a) Density = 35 vehicles/km. (b) Density = 35 vehicles/km. (c) Density = 40 vehicles/km. (d) Density = 40 vehicles/km. (e) Density = 40 vehicles/km. (f) Density = 40 vehicles/km.

5. Comparative analysis of three relevant models

The NaSch model is a classic model widely adopted by scholars. In this model, the limiting braking capacity of vehicles is not considered. Some vehicles often suddenly brake due to speed humps or their own front distance being less than their velocities. In the Pottmeier's model, the limiting braking capacity of vehicles is considered. In the improved Pottmeier's model (the present model), slow-to-start rules are introduced. Compared to the original Pottmeier's model, it can be noted that the phase transition from synchronous flow to wide moving jam is obvious for the improved Pottmeier's model. In this section, we discuss the emission results of these three relevant models, which are specifically the present model adopted in this paper,[46] the Pottmeier's model without slow-to-start rules,[29] and the refined NaSch model.[44] The pollutant emission simulation calculation of these three models is calculated under the same conditions, including the same road length, lattice length, and the location and number of speed humps, etc. The only difference is that the vehicle updates its velocity and position according to the rules of the model used.

For some given density, regardless of the number of speed humps, the refined NaSch model has higher CO_2, NO_X, and PM emissions compared to the present model adopted in this paper[46] and the Pottmeier's model without slow-to-start rules,[29] as shown in Figs. 4(a)–4(f). This is because the refined Nasch model does not take into account the vehicle's limited deceleration capacity. Vehicles in the system frequently accelerate or decelerate, resulting in high CO_2, NO_X, and PM emission values. In a free-flow and synchronized flow region, the present model adopted in this paper and the model without slow-to-start rules have the same emissions values such as CO_2, NO_X, and PM. However, in a wide moving jam region ($d_{SJF} \leq d < d_{SJB}$), compared to the Pottmeier model, the present model adopted in this paper has lower emissions values such as CO_2, NO_X, and PM. This is because slow-to-start rules in the present model adopted in this paper result in more and more vehicles parking in place, resulting in more vehicles with their values of acceleration equal to zero compared to the Pottmeier's model without slow-to-start rules. Thus, the present model adopted in this paper also has higher VOC emissions values in this region.

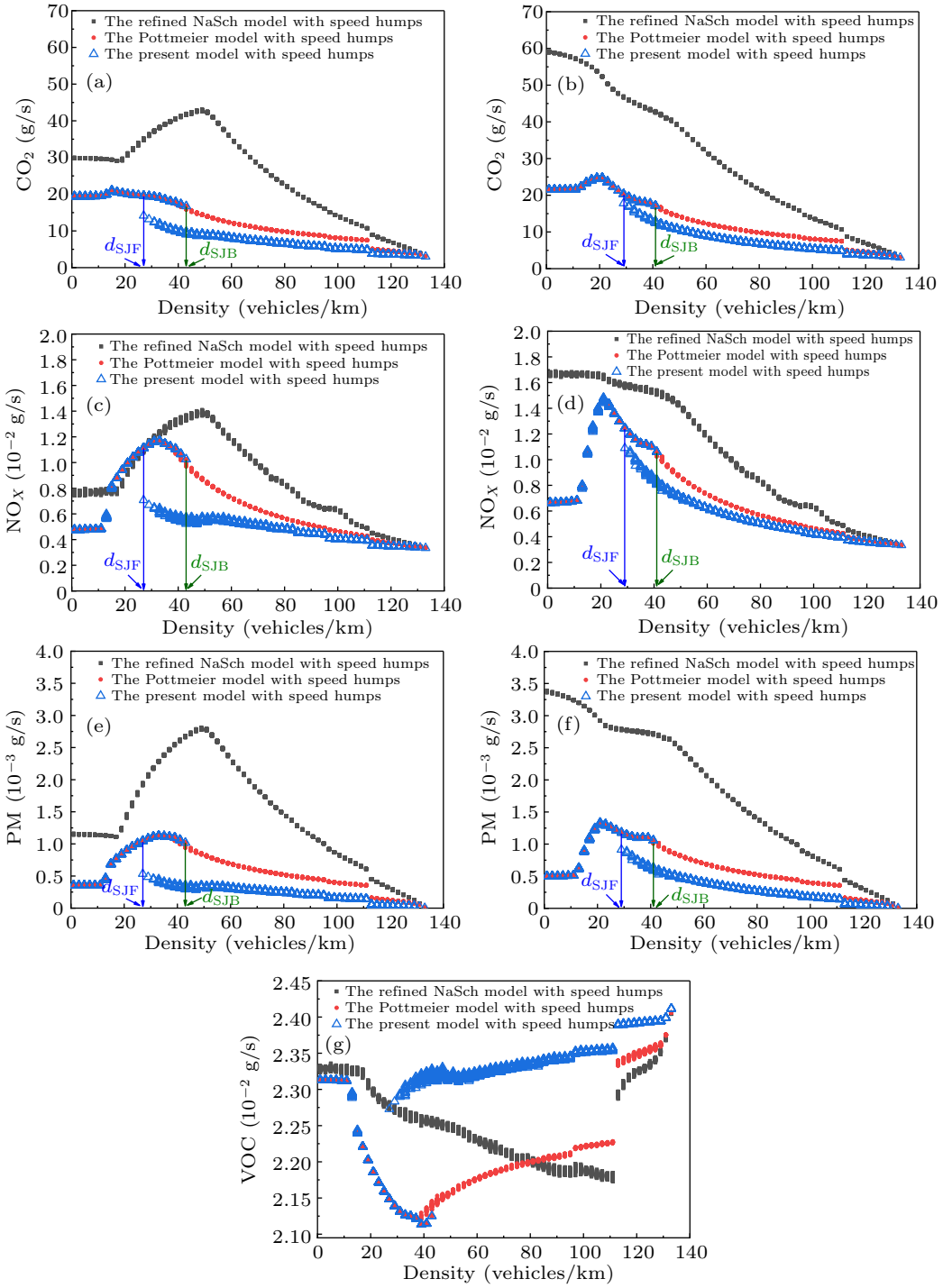


Fig. 4. Comparison of pollutant emissions of three models with different pollutants and speed humps. (a) CO_2 (speed humps = 20), (b) CO_2 (speed humps = 80), (c) NO_X (speed humps = 20), (d) NO_X (speed humps = 80), (e) PM (speed humps = 20), (f) PM (speed humps = 80), (g) VOC (speed humps = 20).

6. Conclusion

Based on the classic instantaneous traffic emission model and the limited deceleration capacity model with slow-to-start rules, this paper has investigated the impact of speed humps on the traffic flow system and the instantaneous emissions of vehicle pollutants in a single lane situation. The numerical simulation results have shown that the value of these pollutant emissions such as CO_2, NO_X and PM is increased by the increase in the number of speed humps in free-flow region ($0 < d < d_{FS}$). However, the opposite situation has occurred for VOC emissions. Moreover, these four pollutant emissions slightly increase or remain unchanged with the increase of vehicle density. Within this range ($d_{SJF} \leq d < d_{SJB}$), these pollutant emissions can evolve into some higher values under some random seeds. Meanwhile, under other random seeds, they can evolve into some lower values. In the wide moving jam region, the emission values of these pollutants appear sometimes as continuous or intermittent phenomenon. These results can be confirmed or explained by the statistical values of velocity

and acceleration.

Compared to the refined NaSch model, the present model (the limited deceleration capacity model with slow-to-start rules) has lower instantaneous emissions such as CO_2, NO_X and PM and higher VOC emissions. Compared to the limited deceleration capacity model without slow-to-start rules, the present model also has lower instantaneous emissions such as CO_2, NO_X and PM and higher VOC emissions in a wide moving jam region. In general, the present model is superior to the two models mentioned. In future research, it can be considered that the limited deceleration capacity model with slow-to-start rules can also be applied to multi-lanes situations and /or heterogeneous traffic flow to better simulate actual instantaneous traffic emissions.

Acknowledgements

This work is funded by the National Natural Science Foundation of China (Grant No. 11875031) and the key research projects of Natural Science of Anhui Provincial Colleges and Universities (Grant No. 2022AH050252).

References

[1] Yang N, Yang L, Xu F, Han X, Liu B, Zheng N Y, Li Y, Bai Y, Li L W and Wang J G 2022 *Sustainability* **14** 16367
[2] Zhao H Y, Wu R L, Liu Y, Cheng J, Geng G N, Zheng Y X, Tian H Z, He K B and Zhang Q 2023 *Environ. Sci. Ecotechnology* **16** 100264
[3] Achakulwisut P, Brauer M, Hystad P and Anenberg S C 2019 *Lancet Planet Health* **3** e166
[4] Zhang K and Batterman S 2013 *Sci. Total Environ.* **450** 307
[5] Dimaratos A, Giechaskiel B, Clairotte M and Fontaras G 2022 *Energies* **15** 5070
[6] Pan S, Du S S, Wang X, Zhang X X, Xia L, Liu J P, Pei F and Wei Y X 2019 *Sustain Cities Soc.* **45** 366
[7] Srimuruganandam B and Nagendra S M S 2010 *Atmos. Pollut. Res.* **1** 184
[8] Wu J B, Guan D X, Yuan F H, Yang H, Wang A Z and Jin C J 2012 *Atmos. Environ.* **61** 9
[9] Chen F Y, Gu X, Yu H M, Zhang X L and Wang Y J 2023 *Environ. Sci. Pollut. Res.* **30** 59540
[10] Hassouna F M A and Assad M 2020 *Int. J. Environ. Res. Public Health* **17** 8940
[11] Huang Q, Hu Y R and Luo L Q 2022 *Environ. Sci. Pollut. Res.* **29** 53293
[12] Derwent R G, Jenkin M E, Utembe S R, Shallcross D E, Murrells T P and Passant N R 2010 *Sci. Total Environ.* **408** 3374
[13] Han S Q, Bian H, Feng Y C, Liu A X, Li X J, Zeng F and Zhang X L 2011 *Aerosol Air. Qual. Res.* **11** 128
[14] Abdel-Wahed T A and Hashim I H 2017 *J. Traffic Transp. Eng. (Engl. Ed.)* **4** 103
[15] Obeng D A, Tuffour Y A, Poku-Boansi M and Amoako C 2022 *Sci. Afr.* **16** e01215
[16] Hassouna F M A, Assad M, Koa I, Rabaya W, Aqhash A, Rahhal A and Saqf-Alhait H 2021 *Atmosphere* **12** 937
[17] Zhou G F, Ma H S, Wang Y F and Cao S Q 2021 *IFAC-Papers On Line* **54** 410
[18] Obregón-Biosca S A 2020 *Results Eng.* **5** 100089
[19] Januševičius T and Grubliauskas R 2019 *Air Qual. Atmos. Health* **12** 635
[20] Baltrėnas H P, Januševičius T and Chlebnikovas A 2017 *Measurement* **100** 62
[21] Nagel K and Schreckenberg M 1992 *J. Phys. I France* **2** 2221
[22] Nagel K and Paczuski M 1995 *Phys. Rev. E* **51** 2909
[23] Takayasu M and Takayasu H 1993 *Fractals* **1** 860
[24] Schadschneider A and Schreckenberg M 1997 *Ann. Phys.* **509** 541
[25] Li X B, Wu Q S and Jiang R 2001 *Phys. Rev. E* **64** 066128
[26] Knospe W, Santen L, Schadschneider A and Schreckenberg M 2000 *J. Phys. A: Math. Gen.* **33** L477
[27] Jiang R and Wu Q S 2003 *J. Phys. A: Math. Gen.* **36** 381
[28] Lee H K, Barlovic R, Schreckenberg M and Kim D 2004 *Phys. Rev. Lett.* **92** 238702
[29] Pottmeier A, Thiemann C, Schadschneider A and Schreckenberg M 2007 *Mechanical restriction versus human overreaction: Accident avoidance and two-lane traffic simulations Traffic and Granular Flow'05* (Springer) pp. 503–508
[30] Kerner B S, Klenov S L and Wolf D E 2002 *J. Phys. A: Math. Gen.* **35** 9971
[31] Li Q L, Wong S C, Min J, Tian S and Wang B H 2016 *Phys. A* **456** 128
[32] Zhao H T, Liu X R, Chen X X and Lu J C 2018 *Phys. A* **494** 40
[33] Singh M K and Rao K R 2020 *IET Intell. Transp. Syst.* **14** 1507
[34] Echab H, Lakouari N, Ez-Zahraouy H and Benyoussef A 2016 *Phys. Lett. A* **380** 992
[35] Madani A and Moussa N 2012 *JATIT £LLS* **35** 250
[36] Li X and Sun J Q 2015 *Phys. A* **438** 251
[37] Wang X, Xue Y, Cen B L, Zhang P and He H D 2020 *Phys. A* **537** 122686
[38] Pan W, Chen X L and Duan X J 2022 *Eur. Phys. J. B* **95** 105
[39] Panis L I, Broekx S and Liu R H 2006 *Sci. Total Environ.* **371** 270
[40] Lakouari N, Oubram O, Bassam A, Hernandez S E P, Marzoug R and Ez-Zahraouy H 2020 *J. Comput. Sci.* **40** 101072
[41] Binoua H, Ez-Zahraouy H, Khallouk A and Lakouari N 2020 *Int. J. Mod. Phy. C* **31** 2050154
[42] Qiao Y F, Xue Y, Wang X, Cen B L, Wang Y, Pan W and Zhang Y X 2021 *Phys. A* **574** 125996
[43] Meng J P and Zhang J F 2006 *Mod. Phys. Lett. B* **20** 835
[44] Pérez-Sansalvador J C, Lakouari N, Garcia-Diaz J and Pomares Hernández S E 2020 *Appl. Sci.* **10** 1592
[45] Kerner B S and Klenov S L 2002 *J. Phys. A: Math. Gen.* **35** L31
[46] Li Q L, Wang J X, Ye L L, Jiang R and Wang B H 2023 *Int. J. Mod. Phy. C* **34** 23050120